Received: 22 March 2020 | Revised: 20 July 2020 | Accepted: 23 July 2020

DOI: 10.1002/bit.27524

ARTICLE

BIOTECHNOLOGY BIOENGINEERING WILEY

Combined genomic and transcriptomic analysis of the dibutyl phthalate metabolic pathway in *Arthrobacter* sp. ZJUTW

Tengfei Liu[1] | **Jun Li**[1] | **Lequan Qiu**[1] | **Fuming Zhang**[2] | **Robert J. Linhardt**[2] | **Weihong Zhong**[1]

[1]College of Biotechnology and Bioengineering, Zhejiang University of Technology, Hangzhou, China

[2]Department of Chemical and Biological Engineering, Center for Biotechnology and Interdisciplinary Studies, Rensselaer Polytechnic Institute, Troy, New York

Correspondence
Weihong Zhong and Lequan Qiu, College of Biotechnology and Bioengineering, Zhejiang University of Technology, 310032 Hangzhou, China.
Email: whzhong@zjut.edu.cn (W. Z.) and lqqiu@zjut.edu.cn (L. Q.)

Funding information
Zhejiang Provincial Natural Science Foundation of China, Grant/Award Number: LY15C010002

Abstract

Dibutyl phthalate (DBP) is an environmental pollutant that can threaten human health. The strain *Arthrobacter* sp. ZJUTW, isolated from the sludge of a river of Hangzhou, can efficiently degrade DBP. Its genomic and transcriptomic differences when cultivated with DBP compared with glucose revealed specific DBP metabolic pathways in the ZJUTW strain. The degrading gene clusters localize separately on a circular chromosome and a plasmid pQL1. Genes related to the initial steps of DBP degradation from DBP to phthalic acid (PA), the *pehA* gene, and *pht* gene cluster, are located on the plasmid pQL1. However, the *pca* gene cluster related to the transforming of intermediate protocatechuic acid (PCA) to acetyl-CoA, is located on the chromosome. After comparative analysis with the reported gene clusters, we found that there were a series of homologous genes in *pht* and *pca* gene clusters that contribute to the efficient degradation of DBP by ZJUTW. In addition, transcriptomic analysis suggested a synergistic effect between *pht* and *pca* clusters, which also favor ZJUTW allowing it to efficiently degrade DBP. Combined genomic and transcriptomic analyses revealed a complete DBP metabolic pathway in *Arthrobacter* sp. ZJUTW that is different from that of other reported *Arthrobacter* strains. After necessary modification based on its metabolic characteristics, *Arthrobacter* sp. ZJUTW or its derivatives might represent promising candidates for the bioremediation of DBP pollution.

KEYWORDS

biodegradation, dibutyl phthalate, genomics, transcriptomics

1 | INTRODUCTION

Phthalic acid esters (PAEs) are important synthetic organic compounds that are often added as plasticizers in plastics and plastic products. As PAEs combine with plastics in the form of noncovalent bonds, PAEs can dissociate from plastic products and be slowly released into the environment when the plastic products are exposed over time to physical factors such as light, weathering, and mechanical forces. As esters with poor aqueous solubility, PAEs accumulate in large quantities in soil and water systems (Wu, Liao, Yu, Wei, & Yang, 2013), causing serious environmental pollution. Studies have shown that PAEs have toxic effects such as carcinogenicity, teratogenicity, mutagenicity and developmental toxicity. Their accumulation in the environment may cause potential substantial harm to human health (Benjamin et al., 2017; Matsumoto, Hirata-Koizumi, & Ema, 2008).

PAEs including DBP, dimethyl phthalate (DMP), diethyl phthalate (DEP), di-n-octyl phthalate, benzyl butyl phthalate (BBP) and

Tengfei Liu and Jun Li contributed equally for the study.

di-(2-ethylhexyl) phthalate (DEHP) have been listed as priority pollutants and environmental endocrine disruptors by the U.S. Environmental Protection Agency (X. Y. Zhang et al., 2014). DBP is the most widely and frequently used PAE (Cheng, Liu, Wan, Yuan, & Yu, 2018). In China, the concentrations of soil accumulated DBP ranged from 0.04 to 29.4 mg/kg (He et al., 2015; Niu, Xu, Xu, Yun, & Liu, 2014). The accumulated DBP may enter plants and eventually the human body through the food chain. Therefore, the elimination of DBP in the environment is crucial for human health.

Removal strategies for pollutants, such as PAEs, usually include hydrolysis, photolysis, and microbial degradation. Recently, the utilization of microorganisms to degrade environmental PAEs has been considered one of the most effective ways for PAEs removal and has resulted in increased attention. For example, Gavala, Alatriste-Mondragon, Iranpour, and Ahring (2003) and Gavala, Yenal, and Ahring (2004) introduced mesophilic anaerobic digestion for treatment of sludge containing PAEs via a process of biodegradation.

An increasing number of PAEs degrading strains belonging to genera *Pseudomonas*, *Gordonia*, *Rhodococcus*, and *Sphingomonas*, have been isolated (Benjamin, Pradeep, Sarath Josh, Kumar, & Masai, 2015; Liang, Zhang, Fang, & He, 2008; Ren, Lin, Liu, & Hu, 2018). However, few DBP degrading strains belonging to genus *Arthrobacter* have been reported. Only a few DBP-degrading *Arthrobacter* stains, *A. keysery* 12B (Eaton, 2001), *Arthrobacter* sp. C21 (Wen, Gao, & Wu, 2014), and *Arthrobacter* sp. ZH2v (Y. Wang, Miao, Hou, Wu, & Peng, 2012) have been isolated from the environment. Until date, the DBP degradation efficiency of these *Arthrobacter* strains is not sufficiently high for their commercial application. Thus, additional novel strains having higher DBP degrading ability are still required.

Recently, a possible metabolic pathway for the biodegradation of PAEs was proposed and divided into three steps (Figure 1): (1) PAEs are converted to PA by the action of a hydrolase; (2) PA is converted to PCA by series of enzymes encoded by the *pht* gene cluster; (3) PCA is transformed into acetyl-CoA, and then enters the tricarboxylic acid (TCA) cycle, and is finally converted to CO_2 and H_2O (Ren, Jia, et al., 2018). However, a complete BDP metabolic pathway is still required for the discovery of new and improved strains.

In our previous study, a novel DBP-degrading strain *Arthrobacter* sp. ZJUTW was isolated from the sludge of a river of Hangzhou, China (Chu, Liu, Zhang, & Qiu, 2017). This organism could degrade and grow on DBP, DEP, and DMP as the sole carbon source under the optimal conditions, 30°C and pH 7.0–8.0. Resting cells could completely degrade 1,200 mg/L of DBP. Thus, we concluded that ZJUTW exhibited a higher capacity of DBP degradation than other organisms described in past publications. However, the mechanism of DBP metabolism needs to be elucidated before the potential application of this organism and its genetic modification to further improve its DBP degrading capacity. Therefore, this study was undertaken to combine comparative genomic and transcriptomic analysis to explore the genes and gene clusters involved in DBP biodegradation and to uncover the complete degradation mechanisms for *Arthrobacter* sp. ZJUTW degradation of DBP.

2 | MATERIALS AND METHODS

2.1 | Chemicals, bacterial strains, and growth conditions

DBP, DMP, DEP, and DEHP were purchased from Yonghua Chemical Co., Ltd. (Jiangsu, China), with a purity greater than 99.5%. Methanol was high-performance liquid chromatography (HPLC) grade and was purchased from Tianjin Siyou Fine Chemicals Co., Ltd. All other reagents were pure analytical grade.

Arthrobacter sp. ZJUTW, isolated from sludge of river of Hangzhou, China had been deposited with the China Center of Typical Culture Collection (CCTCCM2012246).

Luria-Bertani (LB) medium was applied for bacterial enrichment. A modified basic inorganic salt medium (BSM) used for the degradation tests consisted of $K_2HPO_4{\cdot}3H_2O$ 1.0 g, NaCl 1.0 g, $(NH_4)_2SO_4$ 0.5 g, $MgSO_4{\cdot}7H_2O$ 0.4 g, $CaCl_2$ 0.0755 g, and $FeCl_3$ 0.0143 g.

2.2 | DBP degradation by *Arthrobacter* sp. ZJUTW

Arthrobacter sp. ZJUTW strain was inoculated from a slant into 50 ml LB medium in 250 ml sterile Erlenmeyer flask and incubated at 30°C and 180 rpm. After the OD_{600} reached about 0.8, cells were harvested by centrifugation at 4,000 rpm for 10 min. Pellets were washed three times with 0.1 mM phosphate-buffered saline (PBS, pH 7.2), and then re-suspended cells were prepared in an equal volume of BSM. Two milliliters of the suspension (4% inoculum) was inoculated into 50 ml BSM containing different initial DBP

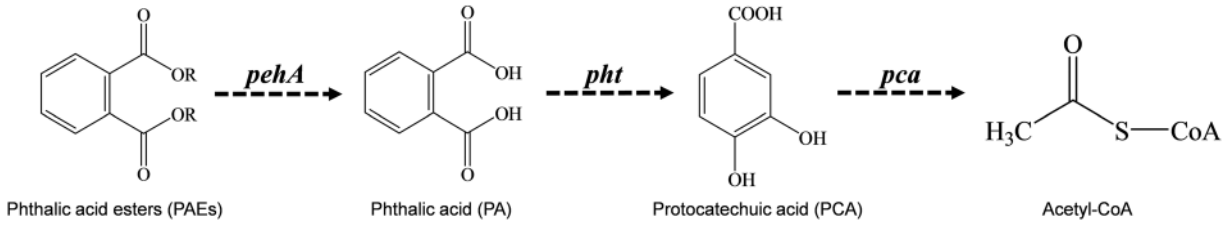

FIGURE 1 Key steps and metabolic intermediates related to PAE biodegradation. PAE, phthalic acid ester; *pca*, the *pca* gene cluster; *pht*, the pht gene cluster; R, different hydrocarbyl groups

concentrations (50,125, 250, 500, and 1,000 mg/L) in a 250 ml sterile Erlenmeyer flask, and then incubated under the optimum conditions (pH 7.0–8.0, 30°C, and 180 rpm). All experiments were performed in triplicate.

The supernatant was collected by centrifugation at 12,000 rpm for 10 min, then mixed with an equal volume of dichloromethane by violent oscillation. The aqueous phase was transferred to a rotary evaporator for drying. The dried substances were dissolved in 2 ml methanol and then filtered through a 0.22 μm membrane filter, the DBP concentration in methanol was measured using an Agilent 1260 HPLC under the following conditions: Diamonsil C18 column, 250 mm × 4.6 mm, 5 μm; the UV wavelength was 235 nm; the mobile phase contained 90% (vol) methanol and 10% (vol) water; the flow rate 1.0 ml/min.

2.3 | Elimination of plasmid

About 0.1 ml of the activated wild-type *Arthrobacter* sp. ZJUTW was inoculated into a 40 ml sterile flask containing 20 ml LB with 0.08 mg/mL sodium dodecyl sulfate (SDS), incubating overnight at 30°C. Then, 100 ml culture medium were smeared on an LB agar plate and cultivated under 30°C for 24 hr to obtain a single colony. Two pairs of primers were used to amplify the 1,407 bp sequence located on the chromosome and the 431 bp sequence located on the plasmid pQL1, which was set as the PCR markers to verify the plasmid removal. The primers for amplifying two sequences are listed in Table S1.

2.4 | Genomic sequencing

Arthrobacter sp. ZJUTW was cultured to the mid-exponential phase in LB medium. Cells were thereby harvested by centrifugation (10,000 rpm, 10 min, 4°C). Genomic DNA was extracted using an EasyPure Bacteria Genomic DNA Kit (TransGenBiotech, Beijing, China). The whole-genome sequencing of the strain ZJUTW was performed using PacBio SMRT. The raw reads were polished by using the SMRT Analysis workflow from Pacific Biosciences to obtain clean reads. The genome of the strain ZJUTW was re-sequenced by an Illumina Hiseq to correct the PacBio results. The complete genome was obtained by sequence assembly using software canu, SPAdes (Bankevich et al., 2012). If there was a group of overlaps with the certain length at both ends of the scaffold assembly, the sequence was looped and one of the overlaps was truncated. Finally, the complete chromosome and plasmid sequences were obtained.

2.5 | Genome annotations

After sequencing, gene prediction of the chromosome was performed using Glimmer 3.02 software (http://ccb.jhu.edu/software/glimmer/index.shtml) and the GeneMarkS (http://opal.biology.gatech.edu/GeneMark/) was used for gene prediction of the plasmid. The predicted gene sequences were performed by sequence alignment with NCBI nr (nonredundant protein database), Swiss-Prot (https://web.expasy.org/docs/swiss-prot_guideline.html), Gene Ontology (GO), and Kyoto Encyclopedia of Genes and Genome (KEGG) databases to obtain functional annotation information. CGview software was used to implement circular genome visualization (Stothard & Wishart, 2005). The rRNA and tRNA contained in the genome were predicted using Barrnap 0.4.2 and tRNAscan-SE v1.3.1 software. A Tandem Repeats Finder was used to predict tandem repeats. Gene Islands (GI) were identified using the IslandViewer program (Bertelli et al., 2017). PHAST (Zhou, Liang, Lynch, Dennis, & Wishart, 2011) and Minced (Bland et al., 2007) were used to find prophages and CRISPR-Cas.

2.6 | Comparative genomic analysis

A total of 25 *Arthrobacter* strains' chromosomes as reference sequences were downloaded from NCBI. The strain ZJUTW was used as a query genome and its genome's circular comparison with 25 strains were performed and visualized using BLAST Ring Image Generator (BRIG, version 0.95; Alikhan, Petty, Ben Zakour, & Beatson, 2011). The specific genes of the strain ZJUTW were identified based on the all-against-all BLASTn alignment results.

The phylogenetic position of ZJUTW among the 26 *Arthrobacter* strains was inferred by using CVTree3 (tlife.fudan.edu.cn/cvtree). According to the phylogenetic tree of 26 strains with fully sequenced genomes, four strains with a close evolutionary relationship were observed. Their orthologous gene determination was based on protein sequence alignment. The BLAST software was used for comparison and extraction of homologous gene pairs ($E < 10^{-5}$). Finally, the orthologous genes and the specific genes in the ZJUTW strain were displayed using a Venn diagram.

2.7 | Mining of genes and gene clusters involved in PAE metabolism

Ester hydrolase and dioxygenase play a key role in PAE degradation. Ester hydrolase is responsible for removing the side chain of PAEs and the ring-cleavage process of aromatic compound results from the action of dioxygenase. Based on the genome sequence obtained and the annotation results, all dioxygenase coding sequences and hydrolase coding sequences were retrieved and manually checked to identify dioxygenases involved in the catabolism of aromatic compounds. The genes of interest (encoding dioxygenase and hydrolase) were located by the Basic Local Alignment Search Tools (BLAST) at the National Center for Biotechnology Information (NCBI). In addition, the upstream and downstream sequences of the target genes were analyzed to identify possible gene clusters. Moreover, to obtain identified genes and gene clusters related to PAE degradation, we reviewed a large body of the relevant literature. The proposed genes and gene clusters were also further analyzed by standalone

blast-2.4.0+ to show their similarity with reported gene clusters, which were retrieved from literature mining.

2.8 | Total RNA isolation and sequencing

For transcriptomic analysis, *Arthrobacter* sp. ZJUTW was inoculated with BSM, supplemented with 0.1% glucose and 400 mg/L (wt/vol) DBP, respectively. After incubation at 30°C and 180 rpm until the broth OD_{600} reached 0.4, the cells were harvested by centrifugation (10,000 rpm, 10 min, 4°C) and immediately mixed with RNA isolator from Vazyme Biotech stored at 80°C for RNA extraction. The quality of extracted RNA was determined by an ND-5000 spectrophotometer and gel electrophoresis. The extracted RNA was sent to Beijing Nuohe Zhiyuan Technology Co., Ltd. for RNA sequencing. The transcriptome sequencing of *Arthrobacter* sp. ZJUTW was performed based on the Illumina sequencing platform. The transcriptomic data were subjected to parametric analysis using *Arthrobacter* sp. ZJUTW as a reference genome. The clean reads were compared to the reference genome or gene sequences using the HISAT2 software and the Bowtie2 software, respectively. The quantitative analysis employed RNA-Seq by Expectation Maximization software based on the alignment results and calculated the expression level of the genes. The analysis of differential expression focuses on finding genes that are differentially expressed between samples and conducting an in-depth analysis of these genes. The differentially expressed genes were further screened for GO and KEGG assignments based on hypergeometric test.

2.9 | Real-time quantitative PCR (RT-qPCR)

The total intracellular RNA of strain ZJUTW was extracted from the control (BSM supplemented with 0.1% glucose) and BSM with 400 mg/L DBP. Strain culture conditions and total RNA isolation was described as RNA-Seq preparation. Total cDNA was then synthesized according to the instruction of a kit HiScript QRT SuperMix (Nanjing Vazyme, China). The transcription level of nine selected genes involved in DBP degradation was measured from three replicates of a single real-time PCR experiment. Each RT-qPCR mixture was prepared via a ChamQ™ Universal SYBR qPCR Master Mix kit (Nanjing Vazyme, China). The RT-qPCR was conducted in a CFX Connect™ Real-Time System (Bio-Rad). The program of qPCR cycling was set as follows: 95°C for 3 min, followed by 39 cycles of 95°C for 10 s, 58°C for 20 s. The transcription level of 16S rRNA was used as the internal control. All the primers for nine genes are listed in Table S1.

3 | RESULTS

3.1 | Degrading ability of *Arthrobacter* sp. ZJUTW

Strain ZJUTW was capable of rapidly degrading low concentrations of DBP (Figure 2). When the DBP concentration in BSM increased to 1,000 mg/L, strain ZJUTW could still grow rapidly and degrade more than 89.46% of DBP within 18 hr. The DBP degradation rate of strain ZJUTW could reach 49.61 $mg{\cdot}L^{-1}{\cdot}hr^{-1}$. However, ZJUTW could not grow when the DBP concentration increased to 1,200 mg/L (Chu et al., 2017). When the initial concentrations are 50, 125, 250, 500, and 1,000 mg/L (4% inoculum), the DBP degradation rate of the first 3 hours could reach 4.98, 13.70, 24.44, 63.71, and 84.07 $mg{\cdot}L^{-1}{\cdot}hr^{-1}$, respectively. These results suggest that the strain ZJUTW seem to degrade DBP more efficiently when the concentration increased.

The DBP biodegradation reaction is also an enzymatic reaction process. Thus, the effect of the initial DBP concentration on degrading efficiency should meet the first-order kinetic model: $\ln C = -K_t + A$ (C is the concentration of DBP at time t, k is the first-order kinetic constant, and A is a constant) and could be used to predict the removal rate of DBP. The kinetic parameters for initial concentrations of DBP calculated are shown in Figure 2. The degradation process of DBP fitted well with the first-order kinetics model when the DBP initial concentration is from 50 to 1,000 mg/L. The biodegradation half-life of DBP by the strain ZJUTW varied from 2.49 to 7.09 hr. These results also showed that stain ZJUTW exhibited different efficiency for various initial concentrations.

Other reported strains that can efficiently degrade DBP, such as *Rhodococcus* sp. JDC-11 could completely degrade 1 g/L DBP within 24 hr with a degradation rate of 21.33 $mg{\cdot}L^{-1}{\cdot}hr^{-1}$, *Bacillus* sp. (NCIM 5220) could degrade 2.783 g/L of DBP within 72 hr with a degradation rate of 38.61 $mg{\cdot}L^{-1}{\cdot}hr^{-1}$, and *Gordonia* sp. JDC2 could degrade 96% of 400 mg/L DBP within 18 hr with a degradation rate of 21.33 $mg{\cdot}L^{-1}{\cdot}hr^{-1}$. To the best of our knowledge, the ZJUTW strain exhibited the highest degradation rate among all reported DBP-degrading strains (Table 1).

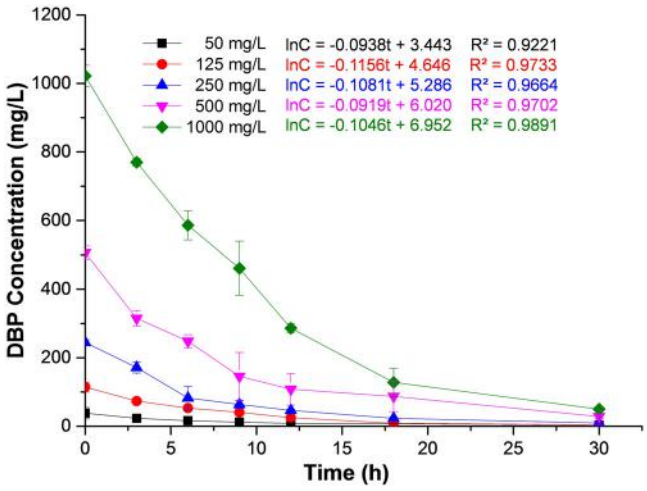

FIGURE 2 Degradation of different initial concentration DBP by *Arthrobacter* sp. ZJUTW in BSM under the optimal conditions: 30°C and pH 8.0. BSM, basic inorganic salt medium; DBP, dibutyl phthalate [Color figure can be viewed at wileyonlinelibrary.com]

TABLE 1 DBP-degrading bacteria strains

Strains	Optimal conditions (pH/temperature)	DBP degradation rate ($mg \cdot L^{-1} \cdot hr^{-1}$)	Performance (degradation efficiencies/time/initial concentration)	References
*Delftia tsuruhatensis*TBKNP-05	7.0/34°C	23.20	100%, 120 hr, 2,783 mg/L	Patil et al. (2006)
Acinetobacter sp. LMB-5	30°C	2.08	100%, 48 hr, 100 mg/L	Fang, Zhang, Wang, Zhou, and Ye (2017)
Acinetobacter lwoffii R3	25°C	16.67	100%, 120 hr, 2,000 mg/L	Hashizume et al. (2002)
Bacillus sp NCIM:5220 (gel entrapped)	7.0/35°C	38.61	100%, 72 hr, 2,783 mg/L	Patil and Karegoudar (2005)
Providencia sp. 2D	8.3/32.4°C	10.74	84.9%, 72 hr, 1,000 mg/L	Zhao et al. (2016)
Methylobacillus sp. V29b	30°C	7.34	70.5%, 192 hr, 2,000 mg/L	Kumar and Maitra (2016)
Pseudomonas sp. V21b	6.8/30°C	5.93	57%, 192 hr, 1,997 mg/L	Kumar et al. (2017)
*Gordonia alkanivorans*YC-RL2	8.0/30°C	0.59	99.4%, 168 hr, 100 mg/L	Nahurira et al. (2017)
Mycobacterium sp. YC-RL4	8.0/30°C	0.42	100%, 120 hr, 50 mg/L	Ren et al. (2016)
Rhodococcus sp. WJ4	7.0/28°C	0.58	97.6%, 168 hr, 100 mg/L	Wang et al. (2015)
Pseudomonas fluoresences FS1	6.5–8.0/30°C	1.39	>99%, 72 hr, 100 mg/L	Zeng, Cui, Li, Fu, and Sheng (2004)
Enterobacter sp. DNB-S2	8.0/35°C	2.97	99.95%, 168 hr, 500 mg/L	Sun et al. (2019)
Bacillus amyloliquefaciens subsp. strain JR20	7.0–8.0/30–40°C	0.047	89.74%, 96 hr, 5 mg/L	Yuan et al. (2019)
Fusarium culmorum	6.5/28°C	5.95	99%, 168 hr, 1,000 mg/L	Ahuactzin-Pérez et al. (2018)
Bacillus mojavensis B1811	6.0–9.0/40°C	5.20	100%, 96 hr, 1,000 mg/L	J. Zhang, Zhang, Zhu, Li, and Li (2018)
Sphingobium yanoikuyae SHJ	7.5/30°C	0.186	50%, 101.4 hr, 50 mg/L	L. Feng, Liu, et al. (2018)
Bacillus megaterium strain YJB3	7.0/34.2°C (Acetate)	1.38	82.5%, 120 hr, 200 mg/L	N.-X. Feng, Yu, et al. (2018)
Sphingobium yanoikuyae TJ	7.0/30°C	15.62	100%, 32 hr, 500 mg/L	D. Jin, Kong, Cui, Bai, and Zhang (2013)
Arthrobacter sp. ZH2	9.0/30°C	10.19	97.82%, 48 hr, 500 mg/L	Wang et al. (2012)
Arthrobacter sp. C21	7.0/30°C	4.28	100%, 70 hr, 300 mg/L	Wen et al. (2014)
Polyporus brumalis	4.5/28°C	0.93	50%, 240 hr, 445 mg/L	Lee et al. (2007)
Gordonia sp. JDC2	7.0/30°C	21.33	96%, 18 hr, 400 mg/L	Wu et al. (2011)
Raoultella sp. ZJY	7.0/30°C	2.49	95.7%, 48 hr, 125 mg/L	Liu, Zhang, Chu, and Qiu (2017)
Ochrobactrum sp. JDC-41	7.0/30°C	7.14	100%, 70 hr, 500 mg/L	Wu, Wang, Liang, Dai, and Chao (2010)
Rhodococcus sp. JDC-11	8.0/30°C (glucose)	41.67	100%, 24 hr, 1,000 mg/L	D. C. Jin et al. (2010)
Gordonia sp. YC-JH1	7.0/30°C	0.81	14%, 24 hr, 139 mg/L	Zhao et al. (2018)
Arthrobacter keysery 12B	ND	ND	ND	Eaton (2001)
Artheobacter sp. ZJUTW	7.0–8.0/30°C	49.61	89.46%, 18 hr, 1,000 mg/L	This study

Abbreviations: DBP, dibutyl phthalate; ND, none detected.

3.2 | Genomic analysis of *Arthrobacter* sp. ZJUTW

The sequencing results showed that the *Arthrobacter* sp. ZJUTW genome contained a chromosome and a plasmid pQL1 (Figure S1). Its genomic nucleotide sequences were submitted to the GenBank databases under accession number CP043624 (chromosome) and CP043625 (plasmid). Genomic features for *Arthrobacter* sp. ZJUTW are provided in Table 2. Using the IslandViewer for genetic transferability analysis, a total of seven gene islands encoding 125 hypothetical proteins, 9 transposase genes, and some other functional proteins were predicted. Prophage prediction was performed by PHAST, a total of 45 genes were predicted, including 36 putative proteins, 1 esterase gene, and 8 other functional proteins. A total of six CRISPR-Cas structures with 32 related sequences were predicted by Minced software.

3.3 | Comparative genomics analysis between ZJUTW and other 25 *Arthrobacter* strains

Twenty-five *Arthrobacter* strains were selected for whole-genome comparison with the strain ZJUTW (Figure S2). A total of 309 specific genes accounting for 8.91% of all ZJUTW genes identified by BLASTp, were found in *Arthrobacter* sp. ZJUTW. Among the 309 specific genes across selected *Arthrobacter* species, 293 genes function was undetermined and the others were transposase genes, *N*-acetyltransferase gene, phosphoesterase gene, HipA-like protein gene, MFS transporter gene, and other functional genes.

The phylogenetic tree analysis results of the whole-genome sequence of 26 strains (Figure 3a) showed that *Arthrobacter* sp. LS16, *Arthrobacter* sp. YC-RL1, and *Arthrobacter* sp. 7749 are phylogenetically closer to ZJUTW than other 22 strains. LS16 is capable of metabolism of phenolic compounds (Hassan et al., 2016). YC-RL1 can efficiently degrade *p*-xylene, naphthalene, phenanthrene, biphenyl, *p*-nitrophenol, and bisphenol (Ren et al., 2018). *Arthrobacter* sp. 7749 can oxidize phenylethanol derivatives (Sastre, Santos, Kagohara, & Andrade, 2017). The protein sequences of LS16, YC-RL1, and 7749 were downloaded from NCBI and were subjected to pairwise alignment using local blast-2.4.0 + software ($E < 10^{-5}$). A Venn diagram (Figure 3b) shows 2,027 homologous genes in the 4 *Arthrobacter* strains and 616 specific genes were found only in stain ZJUTW and not found in the other 3 *Arthrobacter* strains. However, 433 of 616 specific genes are hypothetical protein, the remaining 183 genes are functionally annotated as 1 esterase, 7 ABC transporters, 11 MFS transporters, 9 transposases, transcriptional regulators (GntR, PaaX, HxlR, MerR), and other functional enzymes. The related data are presented in Tables S2 and S3.

TABLE 2 Genomic features of *Arthrobacter* sp. ZJUTW

Features	Chromosome	Plasmid pQL1
Genome size (bp)	3,620,840	52,466
GC content (%)	61.86	57.23
Total number of genes	3,523	71
tRNA	64	0
rRNA	19	0

3.4 | Genes and gene clusters involved in DBP metabolism

Based on the *Arthrobacter* sp. ZJUTW genome annotation results, there are 25 hydrolase genes, 9 esterase genes, and two dioxygenase genes involved in aromatic compounds metabolism. Some gene clusters closely related to biodegradation of DBP, including the *pehA*, *pht* cluster, and *pca* gene cluster, were identified in this study. The *pehA* encodes α/β hydrolase, which can convert DBP to PA, as has been proven in our previous study (Qiu, Zhang, Yin, Liu, & Wu, 2019). The *pht* cluster encodes phthalic acid catabolic enzymes that catalyze the conversion of PA to PCA. The *pca* gene cluster encodes the enzymes catalyzing the transformation of PCA into acetyl-CoA.

3.4.1 | Characteristics of *pht* gene cluster on ZJUTW plasmid pQL1

In the genome of ZJUTW, a *pht* gene cluster was found located on plasmid pQL1. The *pht* gene clusters have been also found in the genomes of other strains including *A. keyseri* 12B (Eaton, 2001), *Gordonia* sp. YC-JH1 (Fan et al., 2018), *Gordonia* sp. HS-NH1 (Li et al., 2016), *Arthrobcter* sp. 68b, *Terrabacter* sp. DBF63 (Habe et al., 2003), and *Mycobacterium vanbaalenii* PYR-1 (Stingley, 2004). However, the gene architecture of the *pht* cluster in *Arthrobacter* sp. ZJUTW is different from that in *Gordonia* sp. YC-JH1 and *A. keyseri* 12B. Each gene of the *pht* gene cluster is adjacent to one another and is aggregated in *A. keyseri* 12B plasmid pRE1 and *Gordonia* sp. YC-JH1. There are *phtAa*, *phtAb*, *phtAc*, *phtAd* coding for 3,4-phthalate dioxygenase on the ZJUTW plasmid pQL1, whereas the *phtAb*, *phtAc*, *phtAd* have two copies. The positions of gene cluster *phtAb1Ac1Ad1* and *phtAaAb2Ac2Ad2* on the plasmid are far away from each other (interval: 12,113 bp), and these two clusters both have the same transcription direction. The *phtB* and *phtC* genes are transcribed in the same direction, but with a distance of 25,325 bp. The transcriptional orientation of gene *phtB* and *phtC* is opposite to that of the two 3,4-phthalate dioxygenase genes mentioned above. The homology alignment analysis with known reports against amino acid sequences of the *pht* cluster of *Arthrobacter* sp. ZJUTW was done and the identities they share with each other are shown in Figure 4a. The gene cluster *phtAaAbAdBC* found in ZJUTW was significantly different from the *pht* gene clusters present in others.

The genes for the initial hydrolysis of DBP are indispensable on plasmid pQL1 (52 kb) of ZJUTW. For example, the putative phthalate (PA) degrading genes encode the essential enzymes for the conversion of phthalic acid to protocatechuic acid, are found on pQL1. PA

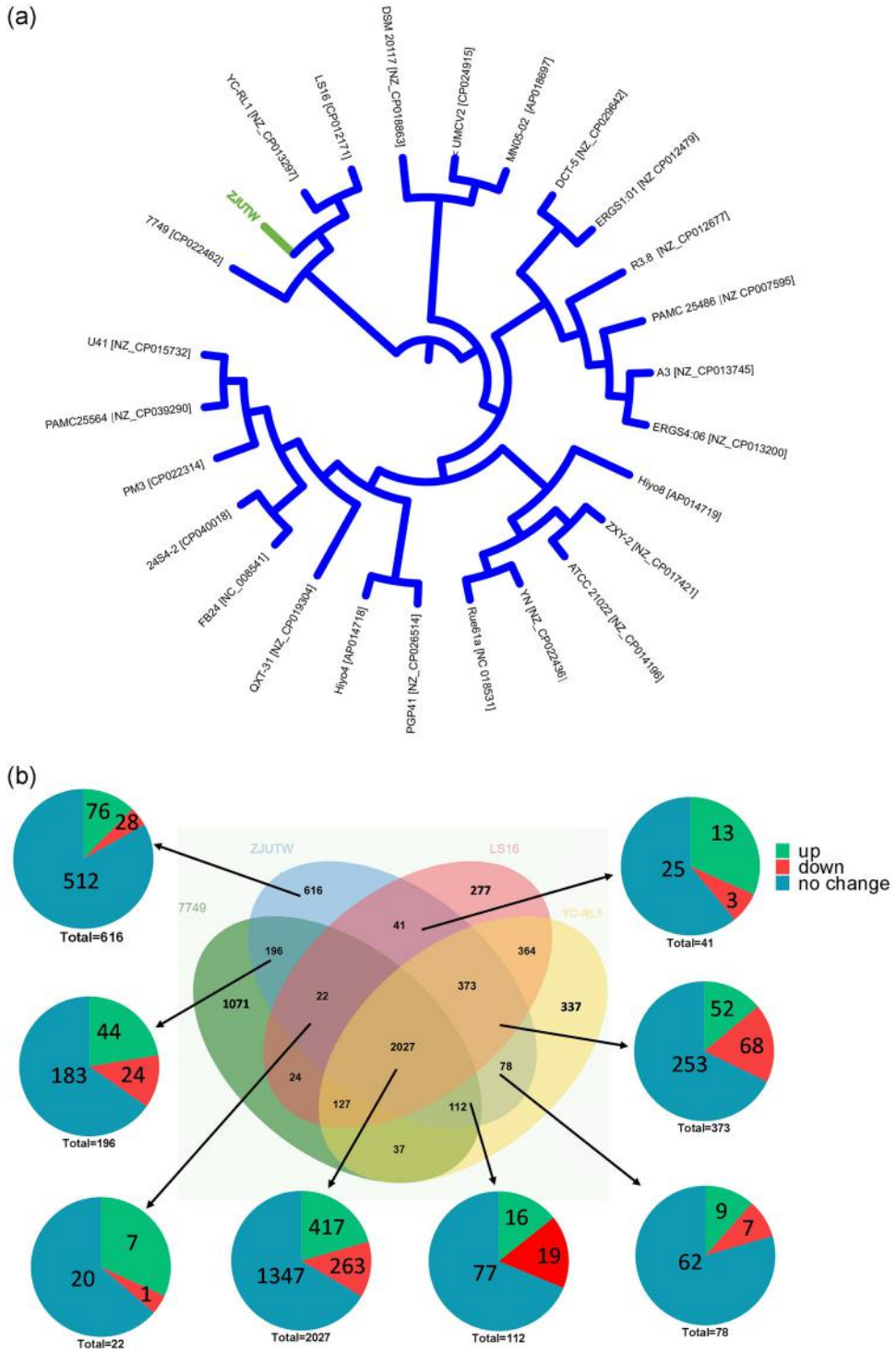

FIGURE 3 The phylogenetic cladogram (a) of ZJUTW with the other 25 available completely sequenced *Arthrobacter* strains, with Venn diagram (b) showing the number of shared and exclusive genes four *Arthrobacter* strains and their differential expression. In (a), GenBank accession numbers following 25 *Arthrobacter* strains names, respectively. For example, Hiyo4 (AP014718) stands for *Arthrobacter* sp. Hiyo4 (AP014718). In (b), the pie chart shows the number of genes with different gene expression level (green, upregulation; red, downregulation; blue, no change) in the corresponding area of the venn diagram [Color figure can be viewed at wileyonlinelibrary.com]

degradation genes were also found on other plasmids including pASPHE302 (94 kb) of *Arthrobacter phenanthrenivorans* Sphe3 (Vandera, Samiotaki, Parapouli, Panayotou, & Koukkou, 2015), pJ340-114 (98 kb) of *Arthrobacter* sp. J3-40, p2MP (112 kb) of *Arthrobacter* sp. 68b (Stanislauskienė et al., 2011), and plasmid 2 (115 kb) of *Arthrobacter* sp. FB24. A synteny comparison analysis between the above-mentioned four plasmids and the plasmid pQL1 showed that pQL1 is obviously different from the other five plasmids. It is the

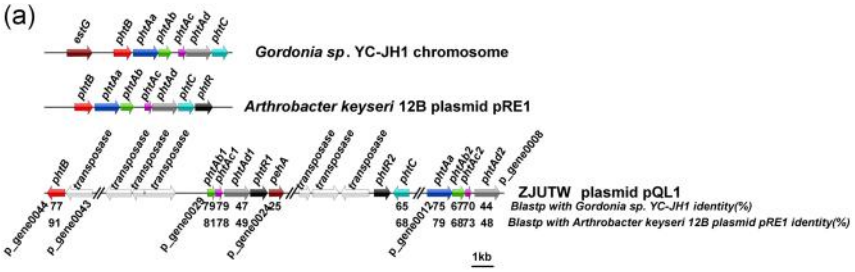
(a)
Gordonia sp. YC-JH1 chromosome
Arthrobacter keyseri 12B plasmid pRE1
ZJUTW plasmid pQL1
Blastp with Gordonia sp. YC-JH1 identity(%)
Blastp with Arthrobacter keyseri 12B plasmid pRE1 identity(%)
1kb

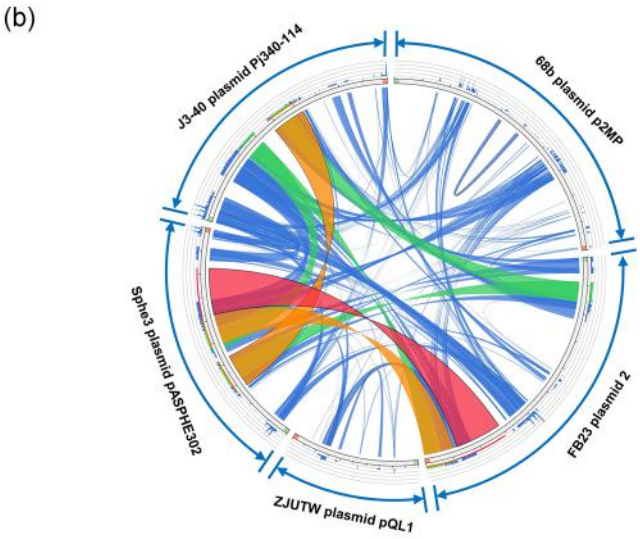
(b)
J3-40 plasmid Pj340-114
68b plasmid p2MP
FB23 plasmid 2
ZJUTW plasmid pQL1
Sphe3 plasmid pASPHE302

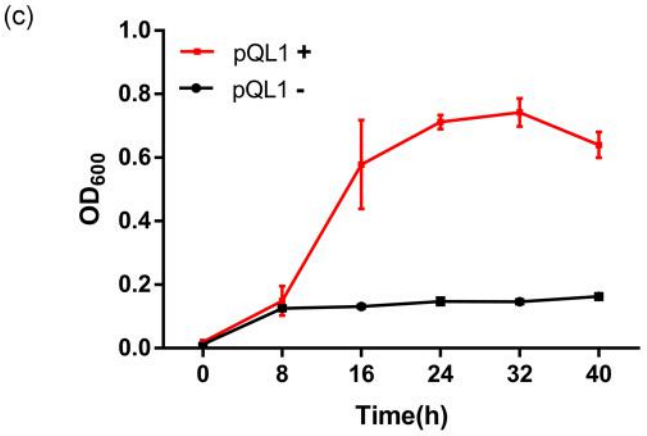
(c)
pQL1 +
pQL1 -
OD600
Time(h)

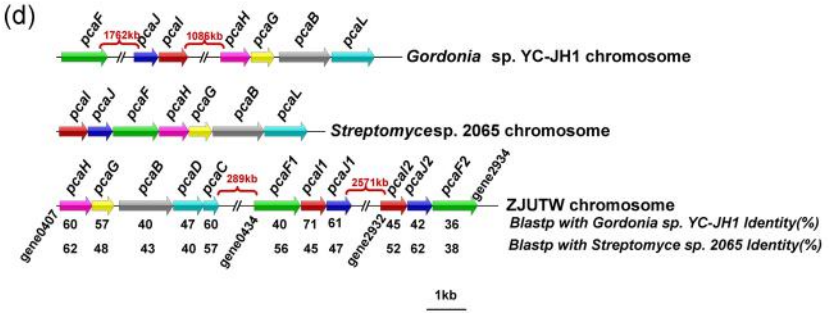
(d)
Gordonia sp. YC-JH1 chromosome
Streptomycesp. 2065 chromosome
ZJUTW chromosome
Blastp with Gordonia sp. YC-JH1 Identity(%)
Blastp with Streptomyce sp. 2065 Identity(%)
1kb

smallest one among the five plasmids and poorly correlated with other plasmids (Figure 4b).

In addition, according to the annotation results of plasmid nucleic acid sequences, we found that there are 12 sequences related to gene transfer on the plasmid, ten of which are annotated as transposase genes and the other two are resolvase, some transposases are very close to the genes in the *pht* gene cluster (Figure 4a). Many of these mobile genetic components are most likely to participate in the shift ingression of the PA decomposition metabolic module, resulting in gene rearrangement and complex mosaic gene structures.

In summary, the whole *pht* gene cluster present in the plasmid pQL1 is very different from all other reported *pht* gene clusters. In addition, the average GC% of the strain ZJUTW chromosome was 61.86%, and that of plasmid pQL1 was 57.23% (Table 2). The plasmid might originate from a possible horizontal gene transfer to facilitate PAE degradation of ZJUTW. Moreover, the *pehA* is also located on the plasmid pQL1, and it is adjacent to *phtR2*. The PehA has been successfully expressed exogenously in BL21 and the enzymatic properties have been determined, including its pH- and thermostability (Qiu et al., 2019). It is a bifunctional enzyme that could both hydrolyze monoesters and diesters. Collectively, the gene *pehA* serves an indispensable role in DBP-degrading.

We obtained a mutant strain of ZJUTW with plasmid removed (Figure S3). The DBP degradation ability and cell growth of wild-type and mutant strains were evaluated from its growth curve (Figure 4c). The plasmid-eliminated strain was prohibited in a stagnant state when DBP was its sole carbon source. Wild type grows more rapidly with an OD_{600} value reaching 0.4 in 12 hr. This suggests that this strain ZJUTW could no longer degrade DBP after plasmid elimination.

3.4.2 | Characteristics of the *pca* gene cluster on ZJUTW chromosome

The gene cluster *pcaHGBCDIJF* involved in the protocatechuic acid (PCA) branch of the 3-ketoadipate pathway, is located on the chromosome of the ZJUTW strain. Specifically, genes *pcaI*, *pcaJ*, and *pcaF* in this cluster have duplicates (i.e. *pcaI1* and *pcaI2*, *pcaJ1*, and *pcaJ2*, *pcaF1* and *pcaF2*) that encode serial enzymes catalyzing the transformation of protocatechuic acid into acetyl-CoA. Of note, some aromatic compound degrading strains, for example, *Streptomyces* sp. 2065 (Iwagami, Yang, & Davies, 2000), *Gordonia* sp. YC-JH1 (Fan et al., 2018), *A. keyseri* 12B, *Arthrobacter* sp. YC-RL1 (Ren et al., 2018) and *Rhodococcus opacus* 1CP (Eulberg, Lakner, Golovleva, & Schlömann, 1998), also bear PCA degradation-related genes in their genomes.

The *pca* gene cluster located on the ZJUTW strain chromosome displays major differences from all other *pca* gene clusters mentioned above. As shown in Figure 4d, the *pca* genes were divided as three parts in the chromosome of the ZJUTW strain, and these three parts are far away from each other. In detail, a 289,334 bp interval between gene cluster *pcaHGBL* and *pcaI1J1F1* was illustrated, whereas a 2,571,339 bp distance for *pcaI1J1F1* compared to *pcaI2J2F2*. The gene cluster *pcaI1J1F1* is closer to gene cluster *pcaHGBCD* compared with the gene cluster *pcaI2J2F2*. The amino acid sequences of the *pca* cluster of *Arthrobacter* sp. ZJUTW share identities of 36–71% and 38–62% with that of *Gordonia* sp. YC-JH1 and *Streptomyces* sp. 2065, respectively. However, the gene cluster responsible for PCA degradation in *A. keyseri* 12B genome is nominated the *pcm* gene cluster, which has the same function to the *pca* gene cluster, while carrying different genes. The *pcm* gene cluster harbors five key genes: *pcmA* (encoding protocatechuic acid 4,5-dioxygenase), *pcmB* (encoding 2-hydroxy-4-carboxymuconic semialdehyde dehydrogenase), *pcmC* (encoding 2-pyrone-4,6-dicarboxylate hydrolase), *pcmD* (encoding 4-oxalomesaconate hydratase) and *pcmE* (4-oxalocitramalate aldolase). Moreover, there is no homology between the *pca* gene clusters in the ZJUTW strain and the *pcm* gene cluster, as analyzed by using BLASTp.

3.5 | Differential transcriptional profile of ZJUTW under DBP and glucose

The transcriptional profile of *Arthrobacter* sp. ZJUTW grown on DBP and glucose was comparatively analyzed using RNA-Seq. Among total

FIGURE 4 Specific genetic architecture of DBP metabolic genes and clusters in strain ZJUTW. (a) The phthalate acid catabolic gene cluster (*pht* gene cluster) of strain ZJUTW locates on its plasmid pQL1 with duplicated homologous genes, while that of *Arthrobacter keyseri* 12B and *Gordonia* sp. YC-JH1, respectively, locates on their plasmid pRE and chromosome, without duplicated homologous genes. (b) Circos plot of full-length synteny comparison for five plasmids. Homologous blocks were presented with identically colored regions and linked across the sequences. (c) ZJUTW lost its DBP degradation capacity when plasmid pQL1 was removed and no growth for mutant without plasmid (pQL1-) was detected when DBP is the sole carbon source in BSM. (d) The protocatechuate catabolic gene cluster (*pca* gene cluster) of *Arthrobacter* sp. ZJUTW locates on its chromosome with duplicated homologous genes, while that of *Gordonia* sp. YC-JH1 and *Streptomyces* sp. 2065 locates on their chromosomes without duplicated homologous genes. BSM, basic inorganic salt medium; DBP, dibutyl phthalate; *pcaB*, 3-carboxy-*cis*,*cis*-muconate cycloisomerase; *pcaC*, 4-carboxymuconolactone decarboxylase; *pcaD*, β-ketoadipate enol-lactone hydrolase; *pcaF*, acetyl-CoA acetyltransferase; *pcaG*, protocatechuate 3,4-dioxygenase α chain; *pcaH*, protocatechuate 3,4-dioxygenase β chain; pcaI, 3-oxoadipate CoA-transferase subunit A; *pcaJ*, 3-oxoadipate CoA-transferase subunit B; *phtAa*, phthalate 3,4-dioxygenase large subunit; *phtAb*, phthalate 3,4-dioxygenase small subunit; *phtAc*, phthalate 3,4-dioxygenase ferredoxin component; *phtAd*, phthalate 3,4-dioxygenase ferredoxin reductase component; *phtB*, 3,4-dihydro-3,4-dihydroxyphthalate dehydrogenase; *phtC*, 3,4-dihydroxyphthalate decarboxylase [Color figure can be viewed at wileyonlinelibrary.com]

2,889 genes detected (including that on chromosome and plasmid), 671 genes were upregulated, 411 genes were downregulated, and 1,807 genes did not change significantly (Figure 5a). A volcano plot of the gene with expression level changed shown that most of *pca* cluster genes fall in the upregulated fields (Figure 5b). Among 671 upregulated and 411 downregulated genes, 122 and 121 genes were significantly upregulated ($\log_2$ fold change ≥ 2.0, $p < 0.05$) and downregulated ($\log_2$ fold change < −2.0, $p < 0.05$), respectively (Table S4).

Among the total of 616 specific genes in the *Arthrobacter* sp. ZJUTW genome, 76 genes were upregulated (Table S5), 28 genes were downregulated (Table S6), and 512 genes did not vary significantly (Figure 3b). It is notable that not all specific areas exhibit significant responses to DBP. Only 4 genes (gene1096, gene2924, gene3435, and gene3054) out of 122 significantly upregulated genes and 7 genes (gene0928, gene0929, gene1081, gene1082, gene1083, gene2294, and gene3144) out of 121 significantly downregulated genes, belong to 616 specific genes. Four significantly upregulated specific genes of the ZJUTW strain, are annotated as hypothetical proteins (gene2924 and gene3435), cupin (gene1096), and α-ketoglutarate transporter (gene3054), respectively. The upregulation of α-ketoglutarate transporter (gene3054) may be a response of ZJUTW to the DBP micro-niche. Gram-positive bacteria have cell walls that contain high levels of peptidoglycans, approximately reaching 90%. When *Arthrobacter* sp. ZJUTW is grown in a BSM with high concentration DBP, its cell wall may be damaged. Peptidoglycan synthesis related genes will be induced to express to adapt to environmental pressure of DBP. Peptidoglycan consists of three parts: the disaccharide unit, tetrapeptide side chain, and peptide interbridge. The tetrapeptide side chain consists of four amino acids, and they are connected to each other by the L- and D-type alternately. As α-ketoglutarate is involved in most L-form amino acid transformations, gene3054 is crucial for the process. Therefore, about five-fold upregulation of gene3054 was detected under DBP stress (Table S4).

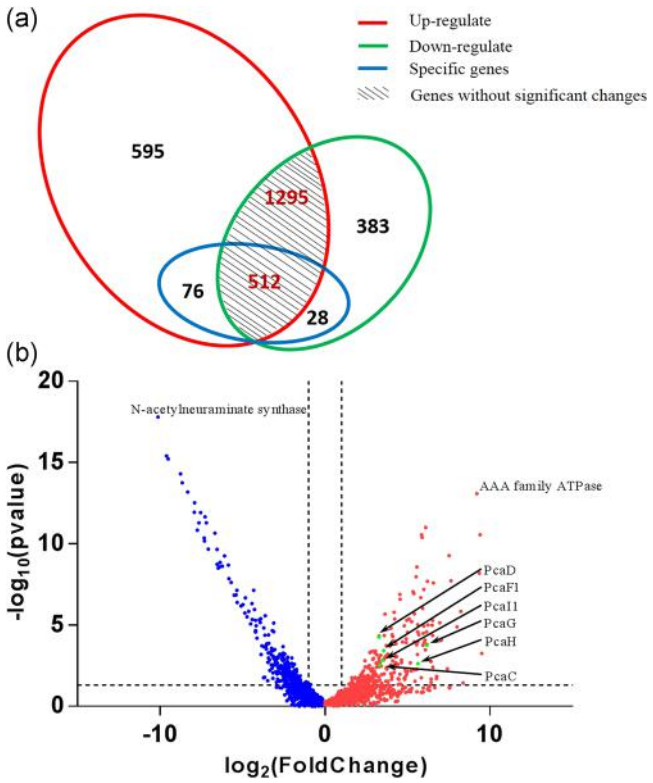

FIGURE 5 Venn diagram (a) and volcano plot (b) showing the gene expression level changes under DBP and glucose carbon sources and the most upregulated and downregulated genes involved in the DBP metabolic process of *Arthrobacter* sp. ZJUTW. In (b), the genes filled in red means that their $\log_2$ (fold change) are positive value, and indicate they are expressed at higher levels in DBP than in glucose. However, the genes filled in blue means that their $\log_2$ (fold change) is negative value, and indicate they are expressed at lower levels in DBP than in glucose. The dotted line on the *x*-axis is obtained when $p = 0.05$. Genes related to DBP degradation are highlighted in green. DBP, dibutyl phthalate [Color figure can be viewed at wileyonlinelibrary.com]

Among the top ten upregulated genes, three are chaperone protein genes (GrpE, DnaK, and GroEL), gene2580 encode ClpB, p_gene0041 encodes an ArsR family transcriptional regulator, gene1281 encodes an anti-sigma factor, and the other four genes encode the MFS (major facilitator superfamily) transporter (gene2727), AAA family ATPase (gene0358), luciferase (gene0604), ATP-dependent chaperone ClpB (gene2580) and NADPH-dependent FMN reductase (gene0678), respectively (Table S7). According to previous publications (Arnau, Sorensen, Appel, Vogensen, & Hammer, 1996; Hartke, Frère, Boutibonnes, & Auffray, 1997; Thomas, Ayling, & Baneyx, 1997), it is known that when cells are exposed to extreme conditions, such as extreme temperatures and arsenite, a series of high-level expressions of hot shock proteins (HSPs), including chaperone proteins, such as GrpE, DnaK, GroEL, and ClpB, are induced. PAEs are toxic to cells when the ZJUTW strain is grown in BSM medium with DBP of high concentrations, the permeability of the cell membrane will be changed, causing damage to the cells, and some functional proteins not to fold appropriately. These factors induce the upregulated MFS (major facilitator superfamily) transporter and a series of chaperone protein (GrpE, DnaK, GroEL, ClpB). Significantly upregulated expression of the MFS transporter gene can be correlated with DBP related efflux. GrpE and DnaK belongs to the HSP70 protein family, GroEL belongs to the HSP60 protein family, and two ClpB belong to the HSP100 protein family. These chaperone proteins fold the newly synthesized peptide chain correctly, repair misfolded polypeptides, degrade the inactive protein, and enable the cells to grow and metabolize normally. Expression of GrpE, DnaK, GroEL chaperone proteins is regulated by the σ32 factor. When the intracellular stress response was reduced, the anti-sigma factor binds and sequester σ32, terminating the sustained transcription of genes coding for these chaperone proteins. This may reason that the expression level of the anti-sigma factor is significantly upregulated. A series of stress responses in the cells is caused by the high concentration of DBP, and these biochemical reactions involve many intracellular redox reactions. We conclude that a significant upregulation of flavin-dependent oxidoreductases and NADPH-dependent FMN reductase genes may be associated with this.

3.6 | Transcription level changes of DBP degrading related genes

The transcription levels of genes located on the *pht* gene cluster and *pca* cluster and alongside *pehA* were measured to obtain a comprehensive understanding of the metabolic process of DBP. As mentioned above, when *Arthrobacter* sp. ZJUTW was cultured in BSM with DBP as the sole carbon source, a total of 122 genes are significantly upregulated (Table S4).

As shown in Table S4, the expression level of the *pehA* (p_gene0024) is upregulated by 2.66-fold compared to the control group. Among the *pht* gene cluster, which comprises *phtAb1*, *phtAc1*, *phtAd1*, *phtR1*, *phtAa*, *phtAb2*, *phtAc2*, *phtAd2*, *phtB*, and *phtC*, the expression level of the *phtAa* (p_gene0012), *phtAb1* (p_gene0029), *phtAd1* (p_gene0026), *phtAb2* (p_gene0011), and *phtB* (p_gene0044) were dramatically upregulated with 3.05-, 3.52-, 4.25-, 3.47- and 5.02-fold, respectively. However, the expression level of *phtAd2* did not change significantly, while the transcription level of *phtC*, *phtAc1* and *phtAc2* was not captured. In summary, these results clearly indicate that the *pehA* and *pht* gene clusters play a significant role in DBP metabolism.

PcaH (the protocatechuic acid 3,4-dioxygenase β-subunit, gene0406), and PcaG (the protocatechuic acid 3,4-dioxygenase α-subunit, gene0407) are protocatechuic acid 3,4-dioxygenases, catalyzing the ring cleavage and the transformation of protocatechuic acid into 3-carboxy-*cis*,*cis*-muconate through ortho-cleavage. Compared to the control group, the expression levels of PcaH and PcaG were upregulated by 6.17-fold and 5.64-fold, respectively. The PcaB (3-carboxy-*cis*,*cis*-muconate cycloisomerase, gene0405), catalyzing conversion of 3-carboxy-*cis*,*cis*-muconate to 4-carboxymuconolactone, was not detected using RNA-Seq-based transcriptomic analysis. The PcaC (4-carboxymuconolactone decarboxylase, gene0403) catalyzes the 4-carboxymuconolactone decarboxylation to form 3-oxoadipate enol-lactone. Its expression is increased by 3.31-fold. The PcaD (gene0404) for the beta-ketoadipate enol-lactone hydrolase can hydrolyze 3-oxoadipate enol-lactone to form the 3-oxoadipate. Its expression level is upregulated by 3.28-fold. Next, the 3-oxoadipate is transformed into acetyl-CoA associated with two key enzymes. One is 3-oxoadipate CoA-transferase, composed of PcaI1 (3-oxoadipate CoA-transferase subunit A) and PcaJ1 (3-oxoadipate CoA-transferase subunit B), 3-oxoadipate is converted to 3-oxoadipyl-CoA by this enzyme. The other one is PcaF1 (acetyl-CoA acetyltransferase), catalyzing the conversion of 3-oxoadipyl-CoA to acetyl-CoA. However, the expression of *pcaF2*, *pcaI12*, and *pcaJ2* was not detected in the transcriptome. This result suggests that *pcaF1*, *pcaI1*, and *pcaJ1* play a leading role in the 3-oxoadipate transformation process.

RT-qPCR analysis on some of the DBP degradation-related genes was performed to confirm the transcriptomic analysis. The RT-qPCR results also show that the expression level of *pehA*, *phtAa*, *pcaD*, *pcaG*, *pcaF1*, and *pcaJ1* were upregulated, consistent with transcriptome data (Figure 6). Combining the results of genomic analysis on the genes and gene clusters involved in DBP degradation and transcriptomic analysis, a possible complete metabolic pathway of DBP in strain ZJUTW could be proposed (Figure 7). In this specific pathway, two ester bonds of DBP are hydrolyzed by α/β-hydrolase (*pehA* encoded) to form PA. PA is then converted to PCA by a series of enzymes encoded by the *pht* gene cluster. Finally, PCA is transferred to acetyl-CoA through related enzymes (*pca* gene cluster encoded). Thus far, only one complete metabolic pathway for DBP in *A. keyseri* 12B has been reported among all *Arthrobacter* strains. In *A. keyseri* 12B, PCA is catalyzed by some enzymes encoded by the gene cluster *pcm*. The *pca* and *pcm* gene clusters encode completely different enzymes (Eaton, 2001). In addition, some key genes in the *pht* and *pca* gene clusters have homologous genes. Overall, the metabolic pathway of DBP in strain ZJUTW is distinct from the pathway in *A. keyseri* 12B.

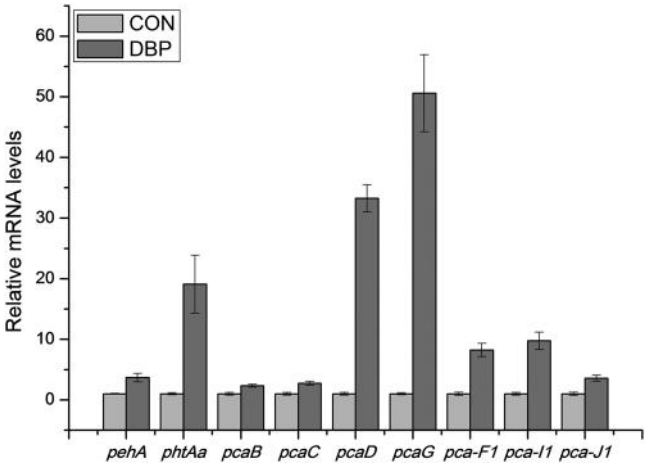

FIGURE 6 Differential expression of genes in the *pht* cluster and *pca* cluster when *Arthrobacter* sp. ZJUTW is grown on glucose (gray) and DBP (black). DBP, dibutyl phthalate

4 | DISCUSSION

4.1 | Specific genetic architecture may contribute to efficiently degradation of DBP by ZJUTW

A large number of DBP-degrading strains have been isolated from the natural environment. For example, *Delftia tsuruhatensis* TBKNP-05 can tolerate and completely degraded 2,783 mg/L DBP in 120 hr (Patil, Kundapur, Shouche, & Karegoudar, 2006), *Bacillus* sp. NCIM:5,220 entrapped in alginate gels can completely degrade 2,783 mg/L DBP in 72 hr (Patil & Karegoudar, 2005), and *Gordonia* sp. JDC2, *Gordonia* sp. JDC13, and *Gordonia* sp. JDC33 were obtained from activated sludge and showed a fair ability to degrade DBP. JDC2 could degrade 96% of 400 mg/L DBP in 18 hr. JDC13 could degrade 98% in 30 hr and JDC33 could degrade 78% in 48 hr (Wu, Wang, Dai, Liang, & Jin, 2011). *Pseudomonas* sp. V21b, isolated from soil, could degrade 57% when the initial concentration of DBP was 1,997 mg/L DBP, within 192 hr (Kumar, Sharma, & Maitra, 2017). When the ZJUTW strain was cultured in BSM containing 1,000 mg/L

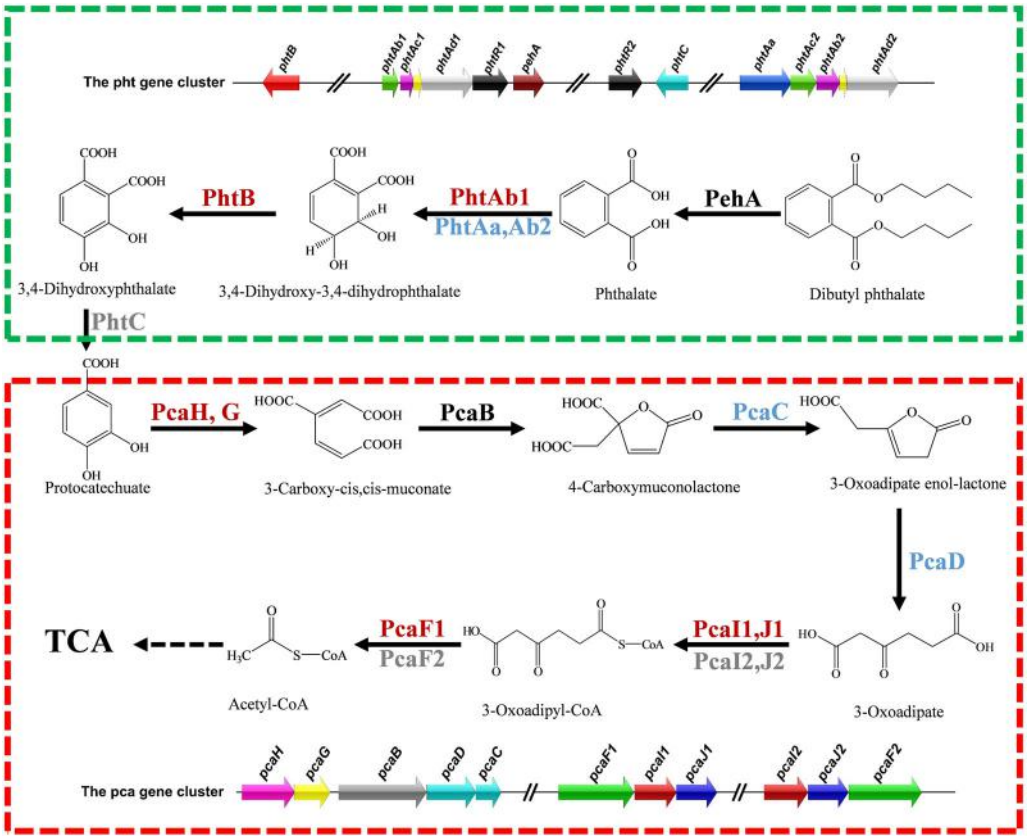

FIGURE 7 Possible metabolic pathways of DBP in strain ZJUTW. Genes were upregulated by 1.50–3.00-fold (black arrows), 3.00–3.50-fold (blue arrows), greater than 3.50-fold (red arrows); genes whose transcripts were not detected via transcriptomics (gray arrows). DBP, dibutyl phthalate; PhtB, phthalic acid ester; TCA, tricarboxylic acid [Color figure can be viewed at wileyonlinelibrary.com]

DBP, it could degrade more than 89.46% of DBP within 18 hr. The DBP degrading rate of the ZJUTW strain was the highest among the reported DBP degrading strains (Table 1).

The highly efficient DBP degradation ability of *Arthrobacter* sp. ZJUTW may be related to the specific genetic architecture of its genome. According to the results of genome sequencing, we found that DBP degradation related gene *pehA*, and gene clusters *pht* and *pca* exhibit a favorable coexisting pattern. As shown in Figure 4a,d, the *pehA* is close to the *pht* gene cluster. In addition, a series of homologous genes were found both in the *pht* and *pca* gene clusters. To our knowledge, the co-occurrence of two homologous gene clusters located on the same plasmid identified in strain ZJUTW is the first report correlated to DBP metabolism. The above two aspects of genetic architecture may play a role in the efficient degradation of DBP by ZJUTW.

To date, the fully reported complete PAEs metabolic pathway in genus *Arthrobacter* is from *Arthrobacter keyseri* 12B (Eaton, 2001). However, its corresponding gene clusters are *pht* and *pcm*. The *pht* gene cluster in *A. keysery* 12B is homologous to that in strain ZJUTW, while the *pcm* gene cluster in strain 12B is not homologous to the *pca* gene cluster in the ZJUTW strain. It other words, PCA is degraded via the β-ketoadipate pathway (*pca* cluster) in strain ZJUTW, while PCA is degraded via the meta-cleavage pathway (*pcm* cluster) in strain 12B. Thus, the DBP metabolic pathway for ZJUTW is distinctly different from that found in *A. keysery* 12B and seems "a new metabolic pathway" in genus *Arthrobacter*.

4.2 | Synergistic effect of the *pht* and *pca* gene clusters may also contribute to efficient degradation of DBP

Arthrobacter sp. ZJUTW exhibited a highly efficient degradation of DBP. This may be closely related to the activity/expression of enzymes encoded by *pht* and *pca* gene cluster, the number of homologous genes, and the location of the two gene clusters in the genome. Some PAEs or PA degrading strains exhibit a different distribution of *pht* and *pca* gene clusters in their genomes. For example, in *A. keyseri* 12B, both of the *pht* gene cluster and gene cluster *pcmDECABF* responsible for PCA metabolism, are located on plasmid pRE1 (Eaton, 2001). In *Mycobacterium vanbaalenii* PYR-1, both the *phtRAaAbAcAd* gene cluster and the *pcaHGBLIJ* gene cluster are located on the chromosome (Stingley, 2004). In *Terrabacter* sp. strain DBF63, the *pht* gene cluster is located on its chromosome while the *pca* gene cluster is unmentioned (Habe et al., 2003). In *Rhodococcus* sp. RHA1, the PA degradation gene clusters are located on two

plasmids pRHL1 and pRHL2 (Hara, Stewart, & Mohn, 2010), while its PCA degradation gene cluster is located on the chromosome (Hara et al., 2010). In *Gordonia* sp. YC-JH1, both of the gene cluster *pcaRGHBLIJF* and *phtRAaAbAcAdBC* are located on the chromosome (Fan et al., 2018). In *A. phenanthrenivorans* Sphe3, two clusters that possibly constitute a phthalic acid catabolism related operon and share an 87% identity with each other, are found on the two plasmids pASPHE301 (190 kb) and pASPHE302 (94 kb; Vandera et al., 2015). Through these comparisons, we show that the distribution of *pht* and *pca* gene cluster on the strain ZJUTW genome is specific to these PAE-degrading strains and each has its own particularity. However, the phenomenon of the two gene clusters, constituting the complete metabolic pathway of a substance, distributed on a chromosome and a plasmid is not a special case in aromatic-degrading strains.

Based on the results of the transcriptome, we compared the transcription level between the genes of the *pht* gene cluster located on the plasmid pQL1 and the genes of the *pca* gene cluster located on the chromosome (Figure 7). The genes related to DBP degradation detected in the transcriptome show different degrees of upregulation. The expression levels of the genes in the *pht* gene cluster were upregulated ranging from 2.66- to 5.02-fold, and the expression levels of the genes in the *pca* gene cluster were upregulated ranging from 2.34- to 6.17-fold. The related data are shown in Table S4. For DBP to be efficiently degraded and to reduce the consumption of energy and certain nutrients, as much as possible, there may be some regulatory mechanism in cells to regulate the transcription of key enzyme genes in the *pht* gene cluster and *pca* gene cluster based on the amount of intracellular substrate and the accumulation of intermediate products.

5 | CONCLUSION

The strain *Arthrobacter* sp. ZJUTW exhibited high degradation efficiency towards DBP. Based on the results of the genome sequencing and the transcriptome, we found the key gene *pehA* and the *pht* gene cluster as well as *pca* gene cluster involved in DBP degradation. The *pehA* gene and *pht* gene cluster are located onto plasmid pQL1, and the *pca* gene cluster is in the chromosome. The genetic particularity of the *pht* and *pca* gene cluster is determined by homology comparison analysis with reported PAEs-degradation gene clusters. The plasmid was successfully eliminated from wild-type ZJUTW by using SDS, and the resultant mutant could not grow in BSM with DBP was as the sole carbon source. The result demonstrates that plasmid pQL1 is critical for the strain ZJUTW to degrade DBP. To the best of our knowledge, we proposed a new complete metabolic pathway from DBP to Acetyl-CoA in the genus *Arthrobacter* for the first time.

ACKNOWLEDGMENTS

This study was supported by the Zhejiang Provincial Natural Science Foundation of China under Grant No. LY15C010002, and for that the authors are grateful.

CONFLICT OF INTERESTS

The authors declare that there are no conflict of interests.

ORCID

Jun Li http://orcid.org/0000-0003-3632-0041

Weihong Zhong http://orcid.org/0000-0002-5673-2222

REFERENCES

Ahuactzin-Pérez, M., Tlecuitl-Beristain, S., García-Dávila, J., Santacruz-Juárez, E., González-Pérez, M., Gutiérrez-Ruíz, M. C., & Sánchez, C. (2018). Mineralization of high concentrations of the endocrine disruptor dibutyl phthalate by *Fusarium culmorum*. *3 Biotech*, *8*(1), 42. https://doi.org/10.1007/s13205-017-1065-2

Alikhan, N.-F., Petty, N. K., Ben Zakour, N. L., & Beatson, S. A. (2011). BLAST ring image generator (BRIG): Simple prokaryote genome comparisons. *BMC Genomics*, *12*(1), 402. https://doi.org/10.1186/1471-2164-12-402

Arnau, J., Sorensen, K. I., Appel, K. F., Vogensen, F. K., & Hammer, K. (1996). Analysis of heat shock gene expression in *Lactococcus lactis* MG1363. *Microbiology*, *142*(7), 1685–1691. https://doi.org/10.1099/13500872-142-7-1685

Bankevich, A., Nurk, S., Antipov, D., Gurevich, A. A., Dvorkin, M., Kulikov, A. S., … Pevzner, P. A. (2012). SPAdes: A new genome assembly algorithm and its applications to single-cell sequencing. *Journal of Computational Biology*, *19*(5), 455–477. https://doi.org/10.1089/cmb.2012.0021

Benjamin, S., Masai, E., Kamimura, N., Takahashi, K., Anderson, R. C., & Faisal, P. A. (2017). Phthalates impact human health: Epidemiological evidences and plausible mechanism of action. *Journal of Hazardous Materials*, *340*, 360–383. https://doi.org/10.1016/j.jhazmat.2017.06.036

Benjamin, S., Pradeep, S., Sarath Josh, M., Kumar, S., & Masai, E. (2015). A monograph on the remediation of hazardous phthalates. *Journal of Hazardous Materials*, *298*, 58–72. https://doi.org/10.1016/j.jhazmat.2015.05.004

Bertelli, C., Laird, M. R., Williams, K. P., Lau, B. Y., Hoad, G., Winsor, G. L., & Brinkman, F. S. (2017). IslandViewer 4: Expanded prediction of genomic islands for larger-scale datasets. *Nucleic Acids Research*, *45*(W1), W30–W35. https://doi.org/10.1093/nar/gkx343

Bland, C., Ramsey, T. L., Sabree, F., Lowe, M., Brown, K., Kyrpides, N. C., & Hugenholtz, P. (2007). CRISPR recognition tool (CRT): A tool for automatic detection of clustered regularly interspaced palindromic repeats. *BMC Bioinformatics*, *8*(1), 209. https://doi.org/10.1186/1471-2105-8-209

Cheng, J., Liu, Y., Wan, Q., Yuan, L., & Yu, X. (2018). Degradation of dibutyl phthalate in two contrasting agricultural soils and its long-term effects on soil microbial community. *Science of the Total Environment*, *640–641*, 821–829. https://doi.org/10.1016/j.scitotenv.2018.05.336

Chu, J., Liu, T., Zhang, H., & Qiu, L. (2017). Screening and characterization of a dibutyl phthalate-degrading bacterium. *Microbiology China*, *44*(7), 1555–1562. https://doi.org/10.13344/j.microbiol.china.170127

Eaton, R. W. (2001). Plasmid-encoded phthalate catabolic pathway in *Arthrobacter keyseri* 12B. *Journal of Bacteriology*, *183*(12), 3689–3703. https://doi.org/10.1128/JB.183.12.3689-3703.2001

Eulberg, D., Lakner, S., Golovleva, L. A., & Schlömann, M. (1998). Characterization of a protocatechuate catabolic gene cluster from *Rhodococcus opacus* 1CP: Evidence for a merged enzyme with 4-carboxymuconolactone-decarboxylating and 3-oxoadipate enol-lactone-hydrolyzing activity. *Journal of Bacteriology*, *180*(5), 1072–1081.

Fan, S., Wang, J., Li, K., Yang, T., Jia, Y., Zhao, B., & Yan, Y. (2018). Complete genome sequence of *Gordonia* sp. YC-JH1, a bacterium efficiently degrading a wide range of phthalic acid esters. *Journal of*

Biotechnology, *279*(January), 55–60. https://doi.org/10.1016/j.jbiotec.2018.05.009

Fang, Y., Zhang, L., Wang, J., Zhou, Y., & Ye, B. (2017). Biodegradation of phthalate esters by a newly isolated *Acinetobacter* sp. strain LMB-5 and characteristics of its esterase. *Pedosphere*, *27*(3), 606–615. https://doi.org/10.1016/S1002-0160(17)60355-2

Feng, L., Liu, H., Cheng, D., Mao, X., Wang, Y., Wu, Z., & Wu, Q. (2018). Characterization and genome analysis of a phthalate esters-degrading strain *Sphingobium yanoikuyae* SHJ. *BioMed Research International*, *2018*, 3917054. https://doi.org/10.1155/2018/3917054

Feng, N.-X., Yu, J., Mo, C.-H., Zhao, H.-M., Li, Y.-W., Wu, B.-X., … Wong, M.-H. (2018). Biodegradation of di-n-butyl phthalate (DBP) by a novel endophytic *Bacillus megaterium* strain YJB3. *Science of the Total Environment*, *616–617*, 117–127. https://doi.org/10.1016/j.scitotenv.2017.10.298

Gavala, H. N., Alatriste-Mondragon, F., Iranpour, R., & Ahring, B. K. (2003). Biodegradation of phthalate esters during the mesophilic anaerobic digestion of sludge. *Chemosphere*, *52*(4), 673–682. https://doi.org/10.1016/S0045-6535(03)00126-7

Gavala, H. N., Yenal, U., & Ahring, B. K. (2004). Thermal and enzymatic pretreatment of sludge containing phthalate esters prior to mesophilic anaerobic digestion. *Biotechnology and Bioengineering*, *85*(5), 561–567. https://doi.org/10.1002/bit.20003

Habe, H., Miyakoshi, M., Chung, J., Kasuga, K., Yoshida, T., Nojiri, H., & Omori, T. (2003). Phthalate catabolic gene cluster is linked to the angular dioxygenase gene in *Terrabacter* sp. strain DBF63. *Applied Microbiology and Biotechnology*, *61*(1), 44–54. https://doi.org/10.1007/s00253-002-1166-6

Hara, H., Stewart, G. R., & Mohn, W. W. (2010). Involvement of a novel ABC transporter and monoalkyl phthalate ester hydrolase in phthalate ester catabolism by *Rhodococcus jostii* RHA1. *Applied and Environmental Microbiology*, *76*(5), 1516–1523. https://doi.org/10.1128/AEM.02621-09

Hartke, A., Frère, J., Boutibonnes, P., & Auffray, Y. (1997). Differential induction of the chaperonin GroEL and the co-chaperonin GroES by heat, acid, and UV-irradiation in *Lactococcus lactis* subsp. lactis. *Current Microbiology*, *34*(1), 23–26. https://doi.org/10.1007/s002849900138

Hashizume, K., Nanya, J., Toda, C., Yasui, T., Nagano, H., & Kojima, N. (2002). Phthalate esters detected in various water samples and biodegradation of the phthalates by microbes isolated from river water. *Biological and Pharmaceutical Bulletin*, *25*(2), 209–214. https://doi.org/10.1248/bpb.25.209

Hassan, I., Eastman, A. W., Weselowski, B., Mohamedelhassan, E., Yanful, E. K., & Yuan, Z.-C. (2016). Complete genome sequence of *Arthrobacter* sp. strain LS16, isolated from agricultural soils with potential for applications in bioremediation and bioproducts. *Genome Announcements*, *4*(1), 4–5. https://doi.org/10.1128/genomeA.01586-15

He, L., Gielen, G., Bolan, N. S., Zhang, X., Qin, H., Huang, H., & Wang, H. (2015). Contamination and remediation of phthalic acid esters in agricultural soils in China: A review. *Agronomy for Sustainable Development*, *35*(2), 519–534. https://doi.org/10.1007/s13593-014-0270-1

Iwagami, S. G., Yang, K., & Davies, J. (2000). Characterization of the protocatechuic acid catabolic gene cluster from *Streptomyces* sp. strain 2065. *Applied and Environmental Microbiology*, *66*(4), 1499–1508. https://doi.org/10.1128/AEM.66.4.1499-1508.2000

Jin, D., Kong, X., Cui, B., Bai, Z., & Zhang, H. (2013). Biodegradation of di-n-butyl phthalate by a newly isolated halotolerant *Sphingobium* sp. *International Journal of Molecular Sciences*, *14*(12), 24046–24054. https://doi.org/10.3390/ijms141224046

Jin, D. C., Liang, R. X., Dai, Q. Y., Zhang, R. Y., Wu, X. L., & Chao, W. L. (2010). Biodegradation of di-n-butyl phthalate by *Rhodococcus* sp. JDC-11 and molecular detection of 3,4-phthalate dioxygenase gene. *Journal of Microbiology and Biotechnology*, *20*(10), 1440–1445. https://doi.org/10.4014/jmb.1004.04034

Kumar, V., & Maitra, S. S. (2016). Biodegradation of endocrine disruptor dibutyl phthalate (DBP) by a newly isolated *Methylobacillus* sp. V29b and the DBP degradation pathway. *3 Biotech*, *6*(2), 200. https://doi.org/10.1007/s13205-016-0524-5

Kumar, V., Sharma, N., & Maitra, S. S. (2017). Comparative study on the degradation of dibutyl phthalate by two newly isolated *Pseudomonas* sp. V21b and *Comamonas* sp. 51F. *Biotechnology Reports*, *15*(April), 1–10. https://doi.org/10.1016/j.btre.2017.04.002

Lee, S.-M., Lee, J.-W., Koo, B.-W., Kim, M.-K., Choi, D.-H., & Choi, I.-G. (2007). Dibutyl phthalate biodegradation by the white rot fungus, *Polyporus brumalis*. *Biotechnology and Bioengineering*, *97*(6), 1516–1522. https://doi.org/10.1002/bit.21333

Li, D., Yan, J., Wang, L., Zhang, Y., Liu, D., Geng, H., & Xiong, L. (2016). Characterization of the phthalate acid catabolic gene cluster in phthalate acid esters transforming bacterium-*Gordonia* sp. strain HS-NH1. *International Biodeterioration and Biodegradation*, *106*, 34–40. https://doi.org/10.1016/j.ibiod.2015.09.019

Liang, D. W., Zhang, T., Fang, H. H. P., & He, J. (2008). Phthalates biodegradation in the environment. *Applied Microbiology and Biotechnology*, *80*(2), 183–198. https://doi.org/10.1007/s00253-008-1548-5

Liu, T. F., Zhang, H. Y., Chu, J. Y., & Qiu, L. Q. (2017). Biodegradation of di-n-butyl phthalate ester by newly isolated *Raoultella* sp. ZJY. *Bulgarian Chemical Communications*, *49*, 104–108.

Matsumoto, M., Hirata-Koizumi, M., & Ema, M. (2008). Potential adverse effects of phthalic acid esters on human health: A review of recent studies on reproduction. *Regulatory Toxicology and Pharmacology*, *50*(1), 37–49. https://doi.org/10.1016/j.yrtph.2007.09.004

Nahurira, R., Ren, L., Song, J., Jia, Y., Wang, J., Fan, S., … Yan, Y. (2017). Degradation of di(2-ethylhexyl) phthalate by a novel *Gordonia alkanivorans* strain YC-RL2. *Current Microbiology*, *74*(3), 309–319. https://doi.org/10.1007/s00284-016-1159-9

Niu, L., Xu, Y., Xu, C., Yun, L., & Liu, W. (2014). Status of phthalate esters contamination in agricultural soils across China and associated health risks. *Environmental Pollution*, *195*, 16–23. https://doi.org/10.1016/j.envpol.2014.08.014

Patil, N. K., & Karegoudar, T. B. (2005). Parametric studies on batch degradation of a plasticizer di-n-butylphthalate by immobilized *Bacillus* sp. *World Journal of Microbiology and Biotechnology*, *21*(8–9), 1493–1498. https://doi.org/10.1007/s11274-005-7369-0

Patil, N. K., Kundapur, R., Shouche, Y. S., & Karegoudar, T. B. (2006). Degradation of a plasticizer, di-n-butylphthalate by *Delftia* sp. TBKNP-05. *Current Microbiology*, *52*(3), 225–230. https://doi.org/10.1007/s00284-005-0258-9

Qiu, L., Zhang, H., Yin, X., Liu, T., & Wu, S. (2019). Properties of a phthalate esters hydrolase from *Arthrobacter* sp. ZJUTW and comparison of its transesterification and ester hydrolysis ability. *Applied Ecology and Environmental Research*, *17*(6), 12937–12949. https://doi.org/10.15666/aeer/1706_1293712949

Ren, L., Jia, Y., Ruth, N., Qiao, C., Wang, J., Zhao, B., & Yan, Y. (2016). Biodegradation of phthalic acid esters by a newly isolated *Mycobacterium* sp. YC-RL4 and the bioprocess with environmental samples. *Environmental Science and Pollution Research*, *23*(16), 16609–16619. https://doi.org/10.1007/s11356-016-6829-4

Ren, L., Jia, Y., Zhang, R., Lin, Z., Zhen, Z., Hu, H., & Yan, Y. (2018). Insight into metabolic versatility of an aromatic compounds-degrading *Arthrobacter* sp. YC-RL1. *Frontiers in Microbiology*, *9*, 2438. https://doi.org/10.3389/fmicb.2018.02438

Ren, L., Lin, Z., Liu, H., & Hu, H. (2018). Bacteria-mediated phthalic acid esters degradation and related molecular mechanisms. *Applied Microbiology and Biotechnology*, *102*(3), 1085–1096. https://doi.org/10.1007/s00253-017-8687-5

Sastre, D. E., Santos, L. P., Kagohara, E., & Andrade, L. H. (2017). Whole-genome sequence of psychrotrophic *Arthrobacter* sp. strain 7749, isolated from antarctic marine sediments with applications in enantioselective alcohol oxidation. *Genome Announcements*, *5*(43), 16–17. https://doi.org/10.1128/genomeA.01197-17

Stanislauskienė, R., Rudenkov, M., Karvelis, L., Gasparavičiūtė, R., Meškienė, R., Časaitė, V., & Meškys, R. (2011). Analysis of phthalate degradation operon from *Arthrobacter* sp. 68b. *Biologija*, *57*(2), 45–54. https://doi.org/10.6001/biologija.v57i2.1828

Stingley, R. L. (2004). Novel organization of genes in a phthalate degradation operon of *Mycobacterium vanbaalenii* PYR-1. *Microbiology*, *150*(11), 3749–3761. https://doi.org/10.1099/mic.0.27263-0

Stothard, P., & Wishart, D. S. (2005). Circular genome visualization and exploration using CGView. *Bioinformatics*, *21*(4), 537–539. https://doi.org/10.1093/bioinformatics/bti054

Sun, R., Wang, L., Jiao, Y., Zhang, Y., Zhang, X., Wu, P., … Yan, L. (2019). Metabolic process of di-n-butyl phthalate (DBP) by *Enterobacter* sp. DNB-S2, isolated from Mollisol region in China. *Environmental Pollution*, *255*, 113344. https://doi.org/10.1016/j.envpol.2019.113344

Thomas, J. G., Ayling, A., & Baneyx, F. (1997). Molecular chaperones, folding catalysts, and the recovery of active recombinant proteins from *E. coli*. *Applied Biochemistry and Biotechnology*, *66*(3), 197–238. https://doi.org/10.1007/BF02785589

Vandera, E., Samiotaki, M., Parapouli, M., Panayotou, G., & Koukkou, A. I. (2015). Comparative proteomic analysis of *Arthrobacter phenanthrenivorans* Sphe3 on phenanthrene, phthalate and glucose. *Journal of Proteomics*, *113*, 73–89. https://doi.org/10.1016/j.jprot.2014.08.018

Wang, J., Zhang, M. Y., Chen, T., Zhu, Y., Teng, Y., Luo, Y. M., & Christie, P. (2015). Isolation and identification of a di-(2-ethylhexyl) phthalate-degrading bacterium and its role in the bioremediation of a contaminated soil. *Pedosphere*, *25*(2), 202–211. https://doi.org/10.1016/S1002-0160(15)60005-4

Wang, Y., Miao, B., Hou, D., Wu, X., & Peng, B. (2012). Biodegradation of di-n-butyl phthalate and expression of the 3,4-phthalate dioxygenase gene in *Arthrobacter* sp. ZH_2 strain. *Process Biochemistry*, *47*(6), 936–940. https://doi.org/10.1016/j.procbio.2012.02.027

Wen, Z. D., Gao, D. W., & Wu, W. M. (2014). Biodegradation and kinetic analysis of phthalates by an *Arthrobacter* strain isolated from constructed wetland soil. *Applied Microbiology and Biotechnology*, *98*(10), 4683–4690. https://doi.org/10.1007/s00253-014-5568-z

Wu, J., Liao, X., Yu, F., Wei, Z., & Yang, L. (2013). Cloning of a dibutyl phthalate hydrolase gene from *Acinetobacter* sp. strain M673 and functional analysis of its expression product in *Escherichia coli*. *Applied Microbiology and Biotechnology*, *97*(6), 2483–2491. https://doi.org/10.1007/s00253-012-4232-8

Wu, X., Wang, Y., Dai, Q., Liang, R., & Jin, D. (2011). Isolation and characterization of four di-n-butyl phthalate (DBP)-degrading *Gordonia* sp. strains and cloning the 3,4-phthalate dioxygenase gene. *World Journal of Microbiology and Biotechnology*, *27*(11), 2611–2617. https://doi.org/10.1007/s11274-011-0734-2

Wu, X. L., Wang, Y. Y., Liang, R. X., Dai, Q. Y., & Chao, W. L. (2010). Degradation of di-n-butyl phthalate by newly isolated *Ochrobactrum* sp. *Bulletin of Environmental Contamination and Toxicology*, *85*(3), 235–237. https://doi.org/10.1007/s00128-010-0080-3

Yuan, L., Cheng, J., Chu, Q., Ji, X., Yuan, J., Feng, F., … Yu, X. (2019). Di-n-butyl phthalate degrading endophytic bacterium *Bacillus amyloliquefaciens* subsp. strain JR20 isolated from garlic chive and its colonization in a leafy vegetable. *Journal of Environmental Science and Health–Part B Pesticides, Food Contaminants, and Agricultural Wastes*, *54*(8), 693–701. https://doi.org/10.1080/03601234.2019.1633211

Zeng, F., Cui, K., Li, X., Fu, J., & Sheng, G. (2004). Biodegradation kinetics of phthalate esters by *Pseudomonas fluoresences* FS1. *Process Biochemistry*, *39*(9), 1125–1129. https://doi.org/10.1016/S0032-9592(03)00226-7

Zhang, J., Zhang, C., Zhu, Y., Li, J., & Li, X. (2018). Biodegradation of seven phthalate esters by *Bacillus mojavensis* B1811. *International Biodeterioration and Biodegradation*, *132*(April), 200–207. https://doi.org/10.1016/j.ibiod.2018.04.006

Zhang, X. Y., Fan, X., Qiu, Y. J., Li, C. Y., Xing, S., Zheng, Y. T., & Xu, J. H. (2014). Newly identified thermostable esterase from *Sulfobacillus acidophilus*: Properties and performance in phthalate ester degradation. *Applied and Environmental Microbiology*, *80*(22), 6870–6878. https://doi.org/10.1128/AEM.02072-14

Zhao, H. M., Du, H., Feng, N. X., Xiang, L., Li, Y. W., Li, H., … Mo, C. H. (2016). Biodegradation of di-n-butylphthalate and phthalic acid by a novel *Providencia* sp. 2D and its stimulation in a compost-amended soil. *Biology and Fertility of Soils*, *52*(1), 65–76. https://doi.org/10.1007/s00374-015-1054-8

Zhao, H. M., Hu, R. W., Chen, X. X., Chen, X., Bin, Lü, H., … Wong, M. H. (2018). Biodegradation pathway of di-(2-ethylhexyl) phthalate by a novel *Rhodococcus pyridinivorans* XB and its bioaugmentation for remediation of DEHP contaminated soil. *Science of the Total Environment*, *640–641*, 1121–1131. https://doi.org/10.1016/j.scitotenv.2018.05.334

Zhou, Y., Liang, Y., Lynch, K. H., Dennis, J. J., & Wishart, D. S. (2011). PHAST: A fast phage search tool. *Nucleic Acids Research*, *39*(suppl), W347–W352. https://doi.org/10.1093/nar/gkr485

SUPPORTING INFORMATION

Additional supporting information may be found online in the Supporting Information section.

How to cite this article: Liu T, Li J, Qiu L, Zhang F, Linhardt RJ, Zhong W. Combined genomic and transcriptomic analysis of the dibutyl phthalate metabolic pathway in *Arthrobacter* sp. ZJUTW. *Biotechnology and Bioengineering*. 2020;117:3712–3726. https://doi.org/10.1002/bit.27524